

Study of the break-up channel in $^{11}\text{Li}+^{208}\text{Pb}$ collisions at energies around the Coulomb barrier

This content has been downloaded from IOPscience. Please scroll down to see the full text.

2014 J. Phys.: Conf. Ser. 515 012004

(<http://iopscience.iop.org/1742-6596/515/1/012004>)

View [the table of contents for this issue](#), or go to the [journal homepage](#) for more

Download details:

IP Address: 129.16.87.152

This content was downloaded on 20/05/2015 at 09:26

Please note that [terms and conditions apply](#).

Study of the break-up channel in $^{11}\text{Li}+^{208}\text{Pb}$ collisions at energies around the Coulomb barrier.

J P Fernández-García^{1,2,3}, M Cubero^{4,5,6}, M Rodríguez-Gallardo¹, L Acosta^{3,7}, M Alcorta², M A G Alvarez^{1,2}, M J G Borge⁴, L Buchmann⁸, C A Diget⁹, H A Falou¹⁰, B R Fulton⁹, H O U Fynbo¹¹, D Galaviz¹², J Gómez-Camacho^{1,2}, R Kanungo¹⁰, J A Lay^{1,13}, M Madurga⁴, I Martel⁷, A M Moro¹, I Mukha¹⁴, T Nilsson¹⁵, A M Sánchez-Benítez^{7,12}, A Shotter¹⁶, O Tengblad⁴, and P Walden⁸

¹ Departamento de FAMN, Universidad de Sevilla, Apartado 1065, E-41080 Seville, Spain.

² Centro Nacional de Aceleradores, Universidad de Sevilla/Junta de Andalucía/CSIC, E-41092 Seville, Spain.

³ Istituto Nazionale di Fisica Nucleare-Laboratori Nazionali del Sud (INFN-LNS), I-95123 Catania, Italy.

⁴ Instituto de Estructura de la Materia-CSIC, E-28006 Madrid, Spain.

⁵ Centro de Investigación en Ciencias Atómicas, Nucleares y Moleculares (CICANUM), CR-2060 San José, Costa Rica.

⁶ Instituto de Física, Universidade Federal Fluminense, Av. Litoranea s/n, Niterói, R.J., Brazil.

⁷ Departamento de Física Aplicada, Universidad de Huelva, E-21071 Huelva, Spain.

⁸ TRIUMF, Vancouver, British Columbia V-6T2A3, Canada.

⁹ Department of Physics, University of York, YO10-5DD Heslington, York, United Kingdom.

¹⁰ Department of Astronomy and Physics, Saint Marys University, Halifax B3H3C3, Canada.

¹¹ Department of Physics and Astronomy, Aarhus University, DK-8000 Aarhus, Denmark.

¹² Centro de Física Nuclear da Universidade de Lisboa (CFNUL), 1649-003 Lisbon, Portugal.

¹³ Dipartimento di Fisica e Astronomia "Galileo Galilei", Università di Padova e INFN, Sezione di Padova, via Marzolo, 8, I-35131 Padova, Italy.

¹⁴ GSI Helmholtzzentrum für Schwerionenforschung GmbH, Planckstr, 1, D-64291 Darmstadt, Germany.

¹⁵ Fundamental Physics, Chalmers University of Technology, S-41296 Gteborg, Sweden.

¹⁶ School of Physics and Astronomy, University of Edinburgh, EH9 3JZ Edinburgh, United Kingdom.

E-mail: fernandez@lns.infn.it

Abstract. We present a study of $^{11}\text{Li}+^{208}\text{Pb}$ collisions at energies around the Coulomb barrier ($E_{lab} = 24.3$ and 29.8 MeV), measured at the post-accelerated beam facility, ISAC II, at TRIUMF (Vancouver, Canada). A remarkably large yield of ^9Li has been observed, a result that is attributed to the weak binding of the ^{11}Li nucleus. The angular distribution of this ^9Li yield, relative to the elastic one, has been analysed in terms of first-order semiclassical calculations as well as four-body and three-body Continuum-Discretized Coupled-Channels (CDCC) calculations, based on a three-body and di-neutron model of the ^{11}Li nucleus, respectively. The calculations reproduce well the trend of the data and support the existence of a large concentration of $B(E1)$ strength at very low excitation energies. The connection of this large $B(E1)$ with a possible low-lying dipole resonance is discussed.

³ Present address: Istituto Nazionale di Fisica Nucleare-Laboratori Nazionali del Sud (INFN-LNS), I-95123 Catania, Italy.



1. Introduction

Since the pioneering experiments with Radioactive Ion Beams (RIB) performed in the 80s at Berkeley by Taninata and collaborators [1], it has been possible to extend the study of stable nuclear reactions to neutron- and proton-rich nuclei. Such developments allow us to investigate the properties of the nuclear interaction, the reaction mechanisms and the nuclear structure of these particular systems, and assess the validity of the structure models developed for stable light nuclei ($N/Z \approx 1$) when the neutron/proton asymmetric increases.

One of the most studied exotic nuclei is ^{11}Li ($N/Z=2.7$). This is an unstable system ($\tau_{1/2}=8.75(13)$ ms [2]), with a Borromean structure consisting of a ^9Li core surrounded by two-weakly bound neutrons ($S_{2n}=369.15(65)$ KeV [3]), in which none of the binary subsystems (n-n or $^9\text{Li-n}$) is bound. The remarkably large reaction cross section observed by Tanihata in 1985 for this nucleus, was interpreted by Hansen and Jonson as due to a high probability of the outermost neutrons to be at large distances from the ^9Li core, which they referred to as a halo structure [4]. A Glauber analysis of ^{11}Li elastic data on protons at intermediate energies yielded a matter radius of 3.62(19) fm [5], significant larger than that obtained in the same experiment for the ^9Li nucleus (2.43(7) fm). We can refer also to the halo size, which is estimated in the same reference as 6.54 fm, and is comparable to the size of the much heavier ^{208}Pb nucleus.

As a consequence of its weak binding, neutron-halo nuclei exhibit a large $B(E1)$ strength at low excitation energies. In the case ^{11}Li , this has been experimentally confirmed by several Coulomb dissociation experiments in complete kinematics [6–9]. Several theoretical calculations have also confirmed this low-lying large $B(E1)$ strength [10–16].

Due to this large $B(E1)$ at small excitation energies, the ^{11}Li nucleus can be easily polarized (and eventually broken-up) by a strong external electric field, such as that produced by a heavy target nucleus. This can be understood because the ^9Li core, positively charged, will move in the field direction, while the weakly-bound neutrons of the halo will not be affected by the electric field. This effect shows up as a strong reduction of the elastic cross section with respect to the Rutherford cross section accompanied by a larger yield of break-up fragments. These effects have been observed and studied, for example, in $^6\text{He}+^{208}\text{Pb}$ reactions [17–21]. The study of collisions of weakly-bound nuclei provide a very valuable information on the structure of these nuclei and, in particular, on the $B(E1)$ strength.

With the motivation of studying these phenomena in the case of ^{11}Li , in a recent experiment the elastic and inclusive breakup of $^{11}\text{Li}+^{208}\text{Pb}$ was measured for the first time at energies below (24.3 MeV) and around (29.8 MeV) the Coulomb barrier ($V_B \approx 28$ MeV) at the RIB facility of TRIUMF (TRI-University Meson Facility), in Vancouver (Canada) [15, 22]. The data revealed a remarkably large yield of ^9Li , presumably coming from the breakup of the projectile. The angular distribution of the ^9Li cross section, relative to the ^{11}Li cross sections, was compared with first-order semiclassical calculations, based on the theory of Alder and Winther for Coulomb excitation, and it was concluded that, in order to reproduce the magnitude of this observable, a very large $B(E1)$ strength close to the breakup threshold was required, in qualitative agreement with the most recent Coulomb dissociation experiment [9].

These conclusions were corroborated with more sophisticated four-body continuum-discretized coupled-channels (CDCC) calculations, based on a three-body model of the ^{11}Li nucleus. Within this model, the large $B(E1)$ close to the threshold is enhanced due to the presence of a dipole resonance, in agreement with some theoretical works [11, 12, 14].

In this contribution, we describe the referred experiment and present additional calculations based on a simple three-body CDCC calculation, in which the ^{11}Li is described within a simple di-neutron model, with an effective two-neutron separation energy. These calculations are compared with the semiclassical and four-body CDCC calculations presented in Refs. [15, 22].

2. Experimental set-up

The experiment, coded as E1104, was carried out at one of the beam lines of the post-accelerated beam facility, ISAC-II, at TRIUMF with a high beam intensity, around 4300 ions of ^{11}Li per second. As displayed in Fig. 1, the experimental set-up was composed by four silicon telescopes covering the angular range between 10° and 140° (see table 1).

Each telescope system consists on two independent detectors: a thin detector, to measure the energy loss (ΔE) by the nuclear reaction fragments, coupled to a thicker detector, to measure the remaining energy (E) deposited by the fragments. Such set-up allows us to separate different fragments in terms of mass and charge in a bi-dimensional diagram ΔE versus $\Delta E + E$ (see Figs. 2 and 3).

Table 1. Angular range of each telescope system.

Telescope ($\Delta E + E$)	Angular range
T1: DSSSD+PAD	$10^\circ - 40^\circ$
T2: DSSSD+PAD	$30^\circ - 60^\circ$
T3: SSSSD+DSSSD	$50^\circ - 100^\circ$
T4: SSSSD+DSSSD	$90^\circ - 140^\circ$

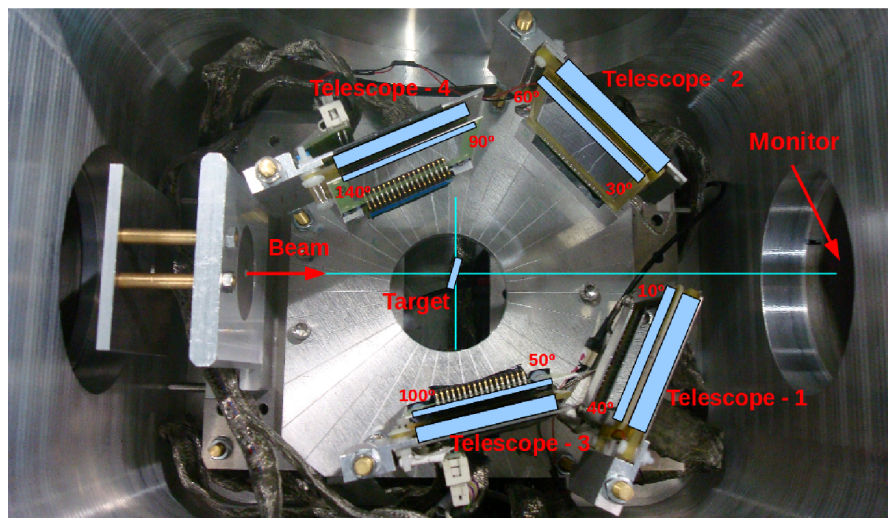


Figure 1. Picture of the experimental setup, with indications of different elements and angles.

The telescopes 1 and 2, covering the forward angles, were composed by a Double Sided Silicon Strip Detector (DSSSD), $40\ \mu\text{m}$ thin detector, and a $500\ \mu\text{m}$ thicker PAD detector. For the backward angles, a $20\ \mu\text{m}$ thin Single Sided Silicon Strip Detector (SSSSD) and a $60\ \mu\text{m}$ thicker DSSSD, were used to form the telescope 3 and 4. Each telescope system was divided into 16 vertical and 16 horizontal strips, that results on 256 pixels. In total, considering four telescopes, our detection system was composed by 1024 ($3 \times 3\ \text{mm}^2$ active area) pixels, which must be considered as independent detectors during the analysis procedure.

To reduce the straggling energy effects, a thin 1.45 mg/cm^2 ^{208}Pb target was used, which was positioned at 75° with respect to the beam direction (see Fig. 1). With these experimental conditions, data were accumulated during 82 hours for the incident energy below the Coulomb barrier, 24.3 MeV, and 119 h for 29.8 MeV incident energy. More details can be found in Refs. [23, 24].

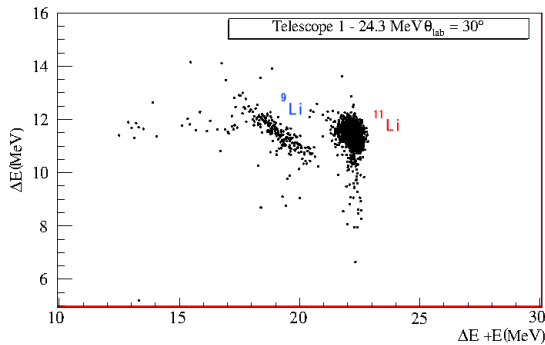


Figure 2. Experimental bi-dimensional diagram for the telescope 1 at the incident energy 24.3 MeV, integrated for the pixels corresponding to the angle $30^\circ \pm 1.5^\circ$.

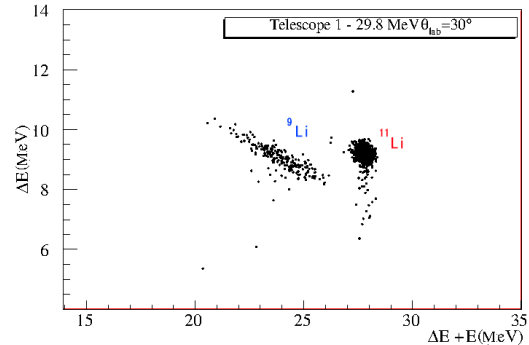


Figure 3. Experimental bi-dimensional diagram for the telescope 1 at the incident energy 29.8 MeV, integrated for the pixels corresponding to the angle $30^\circ \pm 1.5^\circ$.

In Figs. 2 and 3, the data obtained in the reaction $^{11}\text{Li} + ^{208}\text{Pb}$ below and above the Coulomb barrier are shown in the bi-dimensional diagrams ΔE versus $\Delta E + E$ for the telescope 1 integrating all pixels corresponding to the angle $30^\circ \pm 1.5^\circ$. Two different processes, elastic scattering and break-up, are well distinguished.

3. Results and discussion.

The angular distributions of the differential elastic scattering and the break-up cross sections at the two measured energies ($E_{\text{lab}} = 24.3$ and 29.8 MeV) are presented in Figs. 4 and 5, respectively. The latter are represented in terms of the so-called breakup probability, defined as the ratio

$$P_{BU}(\theta) = \frac{N_{BU}(\theta)}{N_{BU}(\theta) + N_{Elast}(\theta)}, \quad (1)$$

where $N_{BU}(\theta)$ and $N_{Elast}(\theta)$ are the number of break-up and elastic events, respectively.

The measured elastic cross section (Fig. 4) exhibits a very strong reduction with respect to the Rutherford prediction, even at energies well below the Coulomb barrier ($V_B \approx 28$ MeV). This behavior is mainly a consequence of the large breakup probability of the ^{11}Li nucleus, as confirmed by the large production of ^9Li observed in the experiment (see Fig. 5).

In order to get further insight into the mechanisms responsible for the suppression of the elastic cross section and the sizable break-up probability, the experimental data are compared with two different theoretical formalisms.

First, semiclassical calculations, performed in Ref. [15] and based on the Alder and Winter approximation of Coulomb excitation [25], were considered. In this model, a classical treatment of the trajectory of the incident particle is considered, while its excitations are treated quantum-mechanically. Due to the large $B(E1)$ strength of ^{11}Li at low excitation energies reported by several Coulomb dissociation experiments [6–9], we expect a dominance of the electric dipole

Coulomb couplings at small angles and/or low incident energies. For a pure $E1$ process, the first-order semi-classical theory gives the break-up probability

$$P_{BU}(E1, \theta) = \left(\frac{Z_A e}{\hbar v a_0} \right)^2 \frac{2\pi}{9} \int_{\varepsilon_b}^{\infty} d\varepsilon \frac{dB(E1)}{d\varepsilon} [I_{1,1}^2(\theta, \varepsilon) + I_{1,-1}^2(\theta, \varepsilon)], \quad (2)$$

where $I_{1, \pm 1}(\theta, \varepsilon)$ are the Coulomb integrals [25] and Z_A the target charge.

The main physical ingredient entering this expression is the $B(E1)$ distribution connecting the ground state of the ^{11}Li nucleus with the continuum states, $dB(E1)/d\varepsilon$. If, for example, the experimental $dB(E1)/d\varepsilon$ obtained by Nakamura *et al* [9] is used, one obtains the result given by the dotted line in Fig. 5. This calculation reproduces well the trend of the data for $\theta_{\text{lab}} \lesssim 40^\circ$ and confirms the dominance of the dipole Coulomb mechanism. However, the magnitude of the breakup probability is somewhat underestimated, suggesting that either *i*) other mechanisms are contributing (e.g. higher-order Coulomb couplings, nuclear breakup, etc) or *ii*) the $dB/d\varepsilon$ strength in ^{11}Li is even larger than that reported by Nakamura *et al*. It is worth noting that these calculations consider only Coulomb couplings and hence they are not expected to be valid at large scattering angles, where nuclear effects are possibly present.

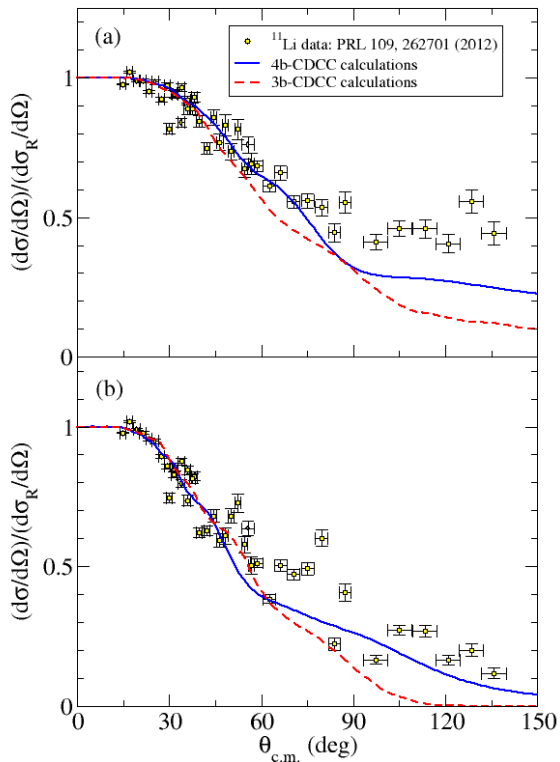


Figure 4. Elastic scattering angular distribution in the center of mass frame at 24.3 (a) and 29.8 (b) MeV.

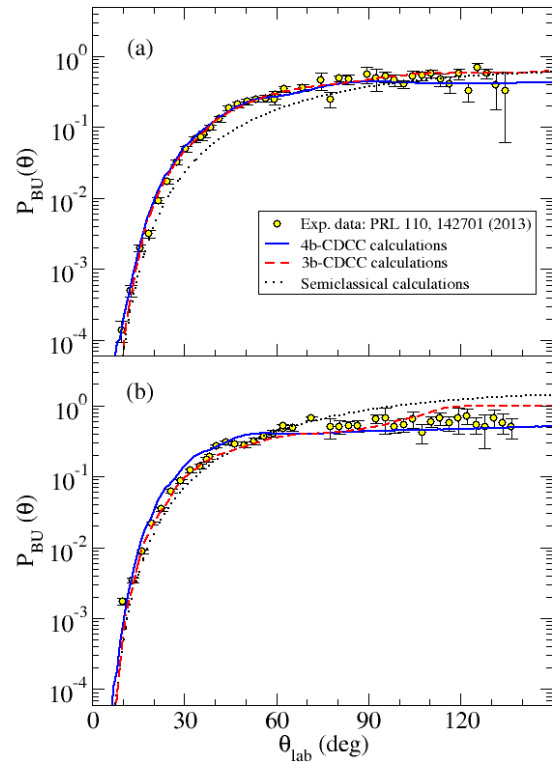


Figure 5. Break-up probability as a function of the laboratory angle at 24.3 (a) and 29.8 (b) MeV.

Since these semiclassical calculations consider only Coulomb couplings, and only to first order, we have performed also more complete three-body (3b) and four-body (4b) CDCC calculations. The CDCC formalism takes into account both nuclear and Coulomb couplings to all orders and hence are not restricted to small angles. Furthermore, the CDCC calculations provide also the

elastic cross sections, in addition to the breakup observables. The four-body CDCC calculations (denoted 4b-CDCC for shortness) make use of a three-body model of ^{11}Li with an inert and spinless ^9Li core. This model gives rise to a low-lying dipole resonance, but its position cannot be accurately predicted by the model, since it depends critically on the effective three-body force required in this model to account for effects beyond the three-body assumption. In particular, for the neutron configuration $J_{nn}^\pi = 0^+$, the strength of the three-body force is adjusted to reproduce the experimental two-neutron separation energy. The three-body CDCC calculations (3b-CDCC hereafter) use a two-body (di-neutron) model for the ^{11}Li nucleus ($^9\text{Li}+2n$). In both cases, the set of coupled equations are solved with the coupled-channels code FRESKO [26].

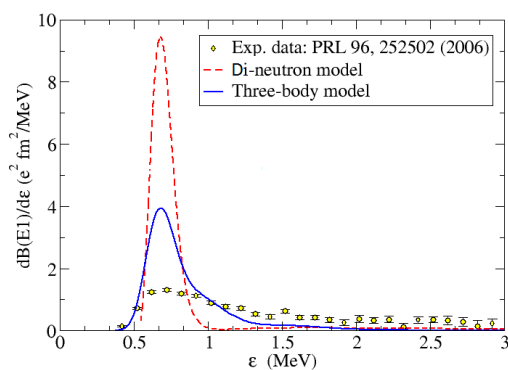


Figure 6. $B(E1)$ distribution of ^{11}Li as a function of the excitation energy.

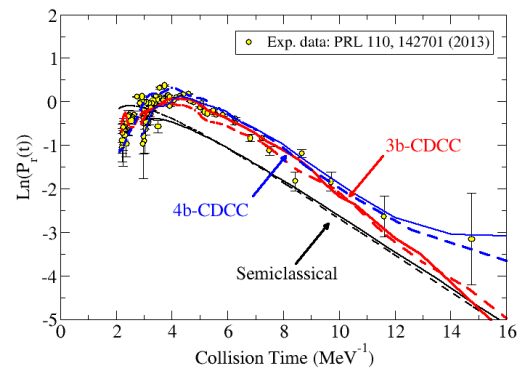


Figure 7. Natural logarithm of the reduced break-up probability as a function of the collision time.

The 4b-CDCC results for the elastic and breakup cross sections are compared with the experimental data in Figs. 4 and 5 (solid lines). As mentioned above, the $B(E1)$ distribution obtained in the three-body model of ^{11}Li (used in the projectile states in the 4b-CDCC calculations) depends critically on the position of the dipole resonance predicted by this model, which can be varied in the model tuning the effective three-body interaction. The calculations shown in Figs. 4 and 5 correspond to the resonance at an excitation energy of $E_x = 0.69$ MeV above the ground state (0.32 MeV above the breakup threshold). With this value, both the elastic cross section and breakup probability are very well described. Thus, the high break-up probability of ^{11}Li can be explained considering a direct break up mechanism. For the 3b-CDCC calculations, the $2n$ - ^9Li interaction was adjusted in order to give the correct rms separation between the center of mass of the two halo neutrons and the core (according to the prediction of the three-body model of ^{11}Li) and a dipole resonance at $E_x = 0.69$ MeV. The results are shown in Figs. 4 and 5 by dashed lines. The breakup probability is also well reproduced, although some underestimation is observed, at backward angles, in the elastic cross sections.

In Fig. 6, the two $B(E1)$ distributions obtained with the di-neutron (red dashed line) and three-body model (blue solid line) of ^{11}Li are compared with the experimental distribution deduced from the latest Coulomb dissociation experiment performed at RIKEN [9]. A large narrow strength at low excitation energies of the $B(E1)$ distributions, considering a di-neutron model of ^{11}Li , is observed. This behavior affects the elastic cross section and the break-up probability, producing the underestimation of the experimental data mentioned before. However, the two models of ^{11}Li , which reproduce the experimental data of Refs. [15] and [22] (Figs. 5 and 4, respectively), suggest more strength of the $B(E1)$ distribution than the one reported from the RIKEN experiment [9].

In general, the breakup probability depends on the structure of the projectile nucleus (^{11}Li in our case) as well as on the characteristics of the reaction (target, energy of the collision, scattering angle, nuclear and Coulomb forces). Thus, disentangling structure information, such as the $B(E1)$ distribution, from the measured cross section is a difficult task. In [15], we proposed a novel procedure that permits constraining the behaviour of the $B(E1)$ distribution in a model-independent way. For that purpose, it is convenient to introduce the so-called *reduced breakup probability*, defined as

$$P_r(t) \equiv P_{BU}(E1, \theta) \frac{9t^2(\hbar v)^3 a_0}{16\pi^2(Z_A e)^2 \sin(\theta/2)}. \quad (3)$$

Within the semiclassical framework, the breakup probability is given by Eq. (2) and hence the reduced breakup probability yields

$$P_r(t) = \int d\varepsilon \frac{dB(E1)}{d\varepsilon} \varepsilon e^{-t\varepsilon} t^2, \quad (4)$$

where t is the so-called *collision time* and is given by the equation

$$t = \frac{a_0}{\hbar v} \left(\pi + \frac{2}{\sin(\theta/2)} \right). \quad (5)$$

So, when the first-order semi-classical approximation is valid, the reduced breakup probability is completely determined by the $B(E1)$ distribution, and is independent on the scattering energy, or the target properties. Expression (4) can be simplified further for small scattering angles (i.e. large collision times) since in that case the exponential appearing in this expression cancels the contribution of large excitation energies and hence the result of the integral is mostly determined by the values of the $B(E1)$ close to the threshold. Approximating the $B(E1)$ by a linear function [15], one can perform the integral explicitly to obtain

$$P_r(t) \approx b e^{-\varepsilon_b t}, \quad (6)$$

where ε_b can be interpreted as an *effective break-up threshold*, while the parameter b is associated with the slope of the $B(E1)$ distribution at low excitation energies. Further details can be found in Ref. [15].

In Fig. 7, the experimental reduced breakup probabilities, obtained from the present breakup data, are compared with the theoretical results, obtained with the 3b-CDCC (red lines) and 4b-CDCC (blue lines) calculations. The solid and dashed lines correspond to the calculations at 24.3 and 29.8 MeV, respectively. The corresponding calculations are in good agreement between themselves and with the experimental data. Calculations and experimental data are very well fitted by the scaling property predicted by Eq. (6) [15]. The reduced breakup probabilities obtained with the semiclassical calculations, making use of the experimental $B(E1)$ distribution of [9], are also shown (black lines) in Fig. 7. These calculations are found to underestimate the experimental reduced breakup probability, thus suggesting that the actual $B(E1)$ strength could be even larger than that reported in Ref. [9].

4. Conclusions

A simultaneous analysis of the elastic and break-up channels of the $^{11}\text{Li}+^{208}\text{Pb}$ reaction at incident energies below (24.3 MeV) and around (29.8 MeV) the Coulomb barrier ($V_B \approx 28$ MeV) has been presented. The weakly bound structure of ^{11}Li gives rises to interesting phenomena in the collision with a heavy target like ^{208}Pb , such as a large suppression of the elastic cross section (with respect to the Rutherford formula) and a large yield of ^9Li fragments. Semiclassical

calculations, based on the first-order theory of Alder and Winther for Coulomb excitation for a pure $E1$ excitation, and whose main ingredient is the $B(E1)$ distribution of ^{11}Li , confirm that the large ^9Li cross section arises from a Coulomb breakup mechanism, mainly due to the strong dipole Coulomb couplings stemming from the strong Coulomb interaction with the heavy target.

The data have been also compared with three-body (3b) and four-body (4b) CDCC calculations. These calculations include explicitly the coupling to the breakup channels due to the Coulomb and nuclear interactions. The 4b-CDCC calculations rely on a pure three-body model of ^{11}Li ($^9\text{Li}+n+n$), while the 3b-CDCC calculations use a simple two-body model ($^9\text{Li}+2n$). These calculations reproduce simultaneously the elastic and breakup data, although the results are very sensitive to the exact location of the dipole resonance in ^{11}Li predicted by this three-body model. Although the total $B(E1)$ strength predicted by the di-neutron model is similar to that obtained in the more realistic three-body model, most of the $B(E1)$ strength is concentrated in the region of the dipole resonance. The 3b-CDCC calculations based on this model reproduce reasonably well the breakup probability and the elastic cross section. Both sets of calculations suggests a large $B(E1)$ strength at low excitation energies, even larger than that obtained from previous Coulomb dissociation experiments [9].

The analysis of the experimental energy and angular distributions of the ^9Li particles coming from the reaction $^{11}\text{Li}+^{208}\text{Pb}$, currently in progress, will allow us to study, in detail, the breakup channels, which will help us to understand better the mechanisms that produce the break-up of the projectile. Due to the difficulties to calculate these observables within a full four-body reaction model, these calculations will be firstly done with the much simpler di-neutron model. These results will be presented elsewhere.

References

- [1] Tanihata I *et al.* 1985 *Phys. Lett. B* **160** 380
- [2] Audi G, Wapstra A H and Thibault C 2003 *Nucl. Phys. A* **729** 337–676
- [3] Smith M *et al.* 2008 *Phys. Rev. Lett.* **101** 202501
- [4] Hansen P G and Jonson B 1987 *Euro. Phys. Lett.* **4** 409
- [5] Egelhof P *et al.* 2002 *Eur. Phys. J. A* **15** 27–33
- [6] Ieki K *et al.* 1993 *Phys. Rev. Lett.* **70** 730
- [7] Shimoura S, Nakamura T, Ishihara M, Inabe N, Kobayashi T, Kubo T, Siemssen R, Tanihata I and Watanabe Y 1995 *Phys. Lett. B* **348** 29–34
- [8] Zinser M *et al.* 1997 *Nucl. Phys. A* **619** 151
- [9] Nakamura T *et al.* 2006 *Phys. Rev. Lett.* **96** 252502
- [10] Korshennikov A A *et al.* 1997 *Phys. Rev. Lett.* **78** 2317–2320
- [11] Ikeda K 1992 *Nucl. Phys. A* **538** 355–365
- [12] Garrido E, Fedorov D V and Jensen A S 2002 *Nucl. Phys. A* **700** 117
- [13] Myo T, Kato K, Toki H and Ikeda K 2007 *Phys. Rev. C* **76** 024305
- [14] Pinilla E C, Descouvemont P and Baye D 2012 *Phys. Rev. C* **85** 054610
- [15] Fernández-García J P *et al.* 2013 *Phys. Rev. Lett.* **110** 142701
- [16] Kikuchi Y, Myo T, Kato K and Ikeda K 2013 *Phys. Rev. C* **87** 034606
- [17] Kakuee O R *et al.* 2006 *Nucl. Phys. A* **765** 294–306
- [18] Sánchez-Benítez A *et al.* 2008 *Nucl. Phys. A* **803** 30
- [19] Escrib D *et al.* 2007 *Nucl. Phys. A* **792** 2–17
- [20] Fernández-García J P, Rodríguez-Gallardo M, Alvarez M A G and Moro A M 2010 *Nucl. Phys. A* **840** 19–38
- [21] Fernández-García J P, Alvarez M A G, Moro A M and Rodríguez-Gallardo M 2010 *Phys. Lett. B* **693** 310–315
- [22] Cubero M *et al.* 2012 *Phys. Rev. Lett.* **109** 262701
- [23] Cubero M *et al.* 2011 *Eur. Phys. J., web of conf.* **17** 16002
- [24] Borge M J G *et al.* 2012 *Journal of Physics: Conf. Series* **381**
- [25] Alder K and Winther A 1975 *Electromagnetic excitation: Theory of Coulomb excitation with heavy ions* (North-Holland)
- [26] Thompson I J 1988 *Computer Physics reports* **7** 167–212